

## FORECASTING FATIGUE LIFE OF HORIZONTALLY CURVED THIN-WALLED BOX-GIRDER RAILWAY BRIDGE EXPOSED TO CYCLIC HIGH-SPEED TRAIN LOADS

### PROCENA ZAMORNOG VEKA TANKOZIDOG HORIZONTALNO ZAKRIVLJENOG SANDUČASTOG NOSAČA ŽELEZNIČKOG MOSTA CIKLIČNO OPTEREĆEN BRZIM VOZOVIMA

Originalni naučni rad / Original scientific paper  
UDK /UDC:

Rad primljen / Paper received: 3.03.2023

Adresa autora / Author's address:

<sup>1)</sup> Faculty of Engineering and Technology, Jain University, Bengaluru, India \*email: [viranjan.v@jainuniversity.ac.in](mailto:viranjan.v@jainuniversity.ac.in)

<sup>2)</sup> Civil Engineering Department, National Institute of Technology, Hamirpur, India

#### Keywords

- box-girder bridge
- bending stresses
- cycle counting method
- fatigue life
- high-speed train

#### Abstract

Damage accumulated through various fatigue processes has a significant impact on the estimated life of a railway bridge exposed to stochastic and variable-amplitude railway vehicle repetitions. There is a critical requirement for monitoring the amount of fatigue damage incurred by bridge superstructures in a timely and precise manner, whether through direct or analytical methods. This study uses the rainflow cycle counting approach to determine the rates of fatigue damage build-up on a horizontally curving, thin-walled box-girder bridge under high-speed train-induced dynamic stress. The thin-walled box-beam finite elements which are computationally effective and consider crucial structural actions like torsional warping, distortion, and distortional warping in addition to the usual displacement and rotational degrees of freedom, have been used to numerically model the curved box-girder bridge. The high-speed train is mathematically simulated using a 38-degree-of-freedom system. The findings indicate the variation of bending stresses for varied bridge lengths, vehicle velocities, and rail surface irregularities. Also, a parametric study has been performed to examine the impact of some critical parameters on the damage index as well as the fatigue life of the curved bridge.

#### INTRODUCTION

The damage accumulated as a result of time varying stresses in a structure is called fatigue. It is likely to take place whenever any structure is exposed to time-varying loads, which in many circumstances can dictate the design. Structures that are exposed to cyclic, repetitive or variable loads can fail under fatigue at substantially lower stress levels than those necessary to produce failure in static conditions. A small amount of damage is done every time a load cycle gets imposed. This type of damage is progressive, meaning it continues to build up until failure. If cracking due to fatigue is identified early, repairing can be done, however, if they are not located and fixed appropriately, the conse-

#### Ključne reči

- sandučasti nosač mosta
- napon savijanja
- metoda brojanja ciklusa
- zamorni vek
- vozovi velikih brzina

#### Izvod

Akumulacija oštećenja tokom različitih procesa zamora ima značajan uticaj na procenu veka železničkog mosta izloženog stohastičkim i ciklusima promenljivih amplituda železničkih vozila. Postoji kritičan zahtev u monitoringu dostignutog oštećenja od zamora, nastalog u superstruktura mostova, definisan vremenski i precizno, bilo putem direktnih ili analitičkih metoda. U radu se koristi metoda kišnog toka za brojanje ciklusa radi određivanja brzina nagomilanog zamornog oštećenja na horizontalno zakrivljenom tankozidom sandučastom nosaču mosta usled dinamičkih napona izazvanih brzim vozom. Konačni elementi tankozidog sandučastog nosača, koji su proračunski efikasni i kojima se uzimaju u obzir ključna naprezanja konstrukcije, kao što su ograničeno uvijanje, izvijanje i izbočavanje, pored uobičajenih pomeranja i stepena slobode rotacije, korišćeni su za numeričko modeliranje zakrivljenog sandučastog profila nosača. Brzi voz se matematički simulira korišćenjem sistema sa 38 stepeni slobode. Rezultati ukazuju na promene napona savijanja za različite dužine mosta, brzine vozila i nepravilnosti površine pruge. Takođe je urađena i parametarska studija kako bi se proučio uticaj nekih kritičnih parametara na indeks oštećenja, kao i na zamorni vek zakrivljene konstrukcije mosta.

quences are severe failures. A bridge is one of the structures that commonly encounters such problems.

Stresses created in structural members of a bridge owing to dynamic interaction with high speed vehicles are not clearly considered in the fatigue provisions in codes of practice for bridge design. The estimated lifespan for a railway bridge exposed to arbitrary railway vehicular cycles, in particular, is highly reliant upon damage accumulated through different mechanisms of fatigue. Bridge component fatigue is typically caused by high cycle fatigue which occurs when the level of stress is substantially lower than what is required to produce failure under a steady state. The current research is carried out to assess damage due to fatigue on curved bridges caused by railway vehicle stress history.

Substantial research on fatigue life prediction has been published in the past by researchers using various methodologies. Fryba /1/ discussed fatigue damage assessments in railway steel bridges. Findings revealed that primary bridge components such as primary girders experience a greater number of cyclic stresses every year. Li et al. /2/ created a model based on fatigue damage to estimate the pattern of damage build-up in a bridge exposed to vehicular stresses. Studies involving fatigue behaviour are performed, and excellent consistency is seen in analytical and experimental findings. Repetto /3/ underlined the importance of defining the limits of fatigue life as a basic requirement in structural design and presented the technique for fatigue analysis caused by wind effect. The cycle counting approach was used by the author, where cycle histograms are represented in closed form. Mohammadi et al. /4/ have focused on utilizing field data to assess and predict the service life of highway bridges. Fifteen steel girder bridges were examined, with a specific focus on fatigue damage in critical structural details. The assessment centered on the superstructure, providing insights into the current condition and fatigue life of each bridge. The study assessed the disparity in fatigue life between a short and medium span bridge caused by consecutive passes of vehicles. Leander and Karoumi /5/ calculated the fatigue life for thick beams using a model built on Timoshenko beam concept. The authors used 22 beams and studied the effect of moving load on them for predicting fatigue life. It was found that dynamic response in continuous beams was at par with the static response and, hence, the dynamic amplification factor came out to be 1.1. Lee et al. /6/ introduced a novel method for predicting the probable fatigue resistance of bridges employing finite element prototype. Parametric findings indicated that the coefficient of correlation had no influence over the anticipated fatigue life of the bridge. Leitner and Figuli /7/ anticipated the fatigue life in mechanical structural components subjected to random stresses. The authors came to the conclusion that material damage is caused by a progressive deterioration process depicted through fatigue damage factor. Macho et al. /8/ devised a framework for determining the expected service life in steel bridges while taking fatigue and corrosion into account. It was established that the adopted technique can result in cost reductions since old bridges could be used for a prolonged period without requiring major restoration. The crack detection in beams subjected to moving mass was identified by Kourehli et al. /9/ by proposing some novel techniques. In the training, verification, and evaluation phases, the authors used artificial neural networks. On the other hand, Bedi and Singh /10/ investigated flexural fatigue life in beams exposed to varying levels of stress. Bertolesi et al. /11/ conducted an analytical and experimental analysis of steel railway bridge fatigue life. According to the findings, fatigue cracks formed around 10 000 cycles and developed rather swiftly until they collapsed at around 31 000 cycles. Kuncham et al. /12/ suggested an online model-based technique for estimating fatigue life using an extended Kalman filter and solely accessible structural health monitoring input. Using the known crack propagation record, the authors calculated the unidentified model parameters and then evaluated crack prognosis based

on these parameters. Su et al. /13/ assessed the fatigue performance in steel bridges using equivalent structural stress. According to the findings, the technique used is a realistic solution to the problem of identifying an appropriate category for measuring fatigue in steel bridges.

Stresses created in structural members of a bridge owing to dynamic interaction with high-speed vehicles are not clearly considered in the fatigue provisions in the codes of practice for bridge design. This is especially true in the context of thin-walled box girder geometries due to the interaction of flexural and torsional stresses which are complemented by cross-section warping and distortion. As per the review of literature, investigations on fatigue life, especially for horizontally curving thin-walled box girder bridges exposed to cyclic high-speed train loads have not yet been explored. Keeping this in mind, extensive research is conducted for estimating fatigue life of a thin-walled box girder bridge based on the high-speed train produced stress history.

#### DIFFERENT VEHICLE-BRIDGE INTERACTION SYSTEM MODELLING

Fatigue life of a curved bridge exposed to a high-speed train is estimated by taking into account the bridge-train-track system's coupled interaction system. The modelling of different associated systems has been discussed in the following sections.

##### *Curved bridge modelling*

Figure 1 depicts a curved thin-walled box beam element with straight lines generating cross-sections. The distortion study is eased by presuming that the cross-section's axis of symmetry remains vertical. In order to do an analysis for torsion and bending, this condition is no longer necessary. The element axis is described as the location of centroids that are eccentric to but parallel to the flexural axis. The axis has three elemental nodes, two at each end and one in the middle. A localized Cartesian coordinate system ( $x, y, z$ ) is being used to represent the element.

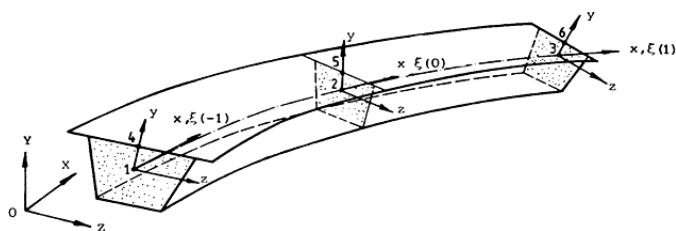


Figure 1. Three-noded thin-walled box beam element.

The centroid of the cross-section symbolises the coordinate system's origin. It is also supposed that the cross-section's primary axis conforms to the local  $yz$  axis orientation. The localized  $x$  axis lies tangent towards the element's axis. The tangent extends from the first node to the third. The vertical symmetrical axis is depicted through localized  $y$  axis, whilst the localized  $z$  axis is expressed by a right handed orthogonal system.

The global coordinate system has been expressed using a natural coordinate  $\xi$ , with values  $-1, 0$  and  $+1$  over three elemental faces. If 'P' represents a point over the element's axis and  $r = X.i + Y.j + Z.k$  is its position vector, then a unit tangent vector in the  $x$  direction can be written as:



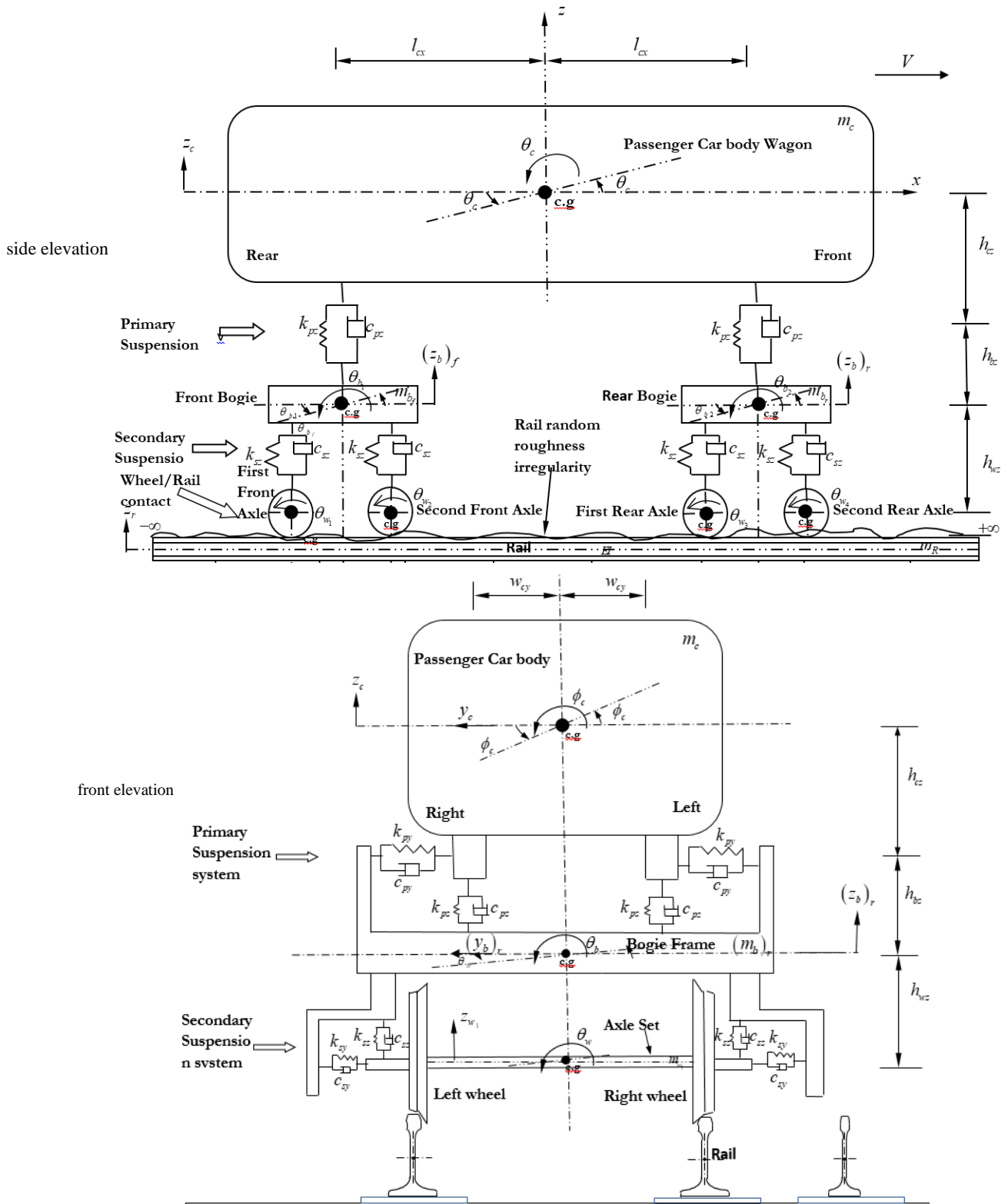


Figure 2. High speed train model.

Table 1. Vehicle system with 38 degrees of freedom.

DOF	yaw	sway	heave	pitch	roll	surge
Component						
Car body	$x_c$	$y_c$	$z_c$	$\theta_c$	$\phi_c$	$\psi_c$
Bogie (front and rear)	$x_b$	$y_b$	$z_b$	$\theta_b$	$\phi_b$	$\psi_b$
Wheel sets (four)	$x_w$	$y_w$	$z_w$	-	$\phi_w$	$\psi_w$

Experiment for fatigue strength

For fatigue assessment, both the material characteristics as well as the dynamic load procedure are critical. Periodic load, described as a steady amplitude load cycle, is the most basic among all fatigue load procedures. The empirical studies from these constant amplitude experiments serve as a starting point for predicting fatigue life in complex time

histories. Steady fatigue behaviour is predicted using experiments that regulate and vary a load or deflection in a simple periodic way till failure. In such a case, fatigue failure is seen to be highly dependent on the stress range, which can be expressed as the difference of peak- and lowest stress. An alternate approach employs the average stress value, described as the mean of the least and greatest stress levels. In most cases, the stress range effect is proven to be far more relevant as compared to average stress. Figure 3 depicts a standard stress history under constant amplitude load.

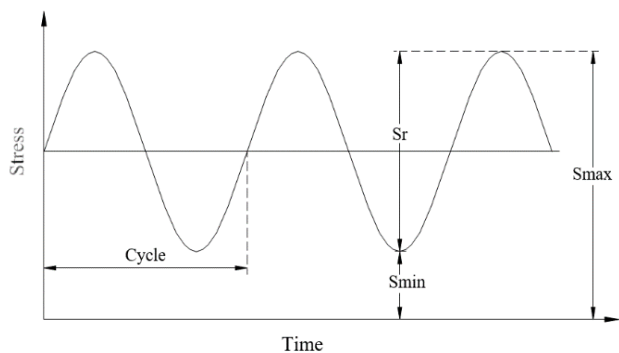


Figure 3. Stress history under constant amplitude load.

The outcome of steady amplitude fatigue analysis is frequently expressed through stress range  $S_r$  and the number of cycles before failure  $N_f$ . A standard experimental evaluation of steady amplitude fatigue for a particular design and material includes a series of tests. As illustrated in Fig. 4, the findings of the tests are often given in the form of an S-N curve.

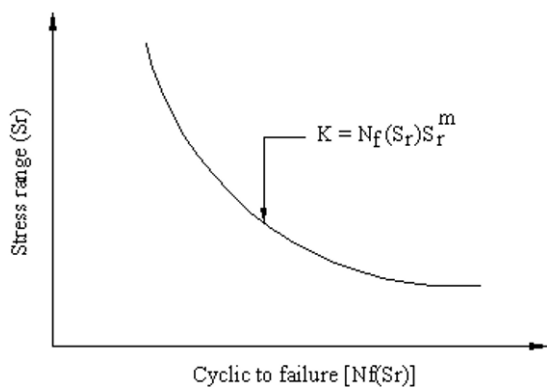


Figure 4. A standard S-N curve.

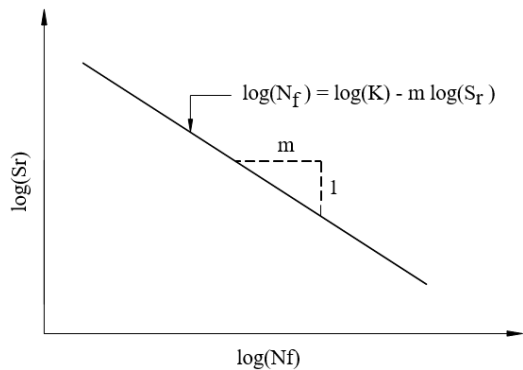


Figure 5. S-N curve over log-log plot.

Typically, experimental analysis reveals that a considerable section of the S-N curve may be put into an equation given by:

$$N_f S_r = K S_r^{-m}, \tag{19}$$

where:  $K$  and  $m$  represent material constants.

The S-N curve can be represented over a log-log plot, Fig. 5, by the equation below:

$$y = c + ax, \tag{20}$$

where:  $y = \log(N_f)$ ;  $c = \log(K)$ ;  $a = -m$ ;  $x = \log(S_r)$ .

*Cycle counting method*

The process of converting time history of the loading into a series of cycles is termed as cycle counting. Throughout literature, there are several statistical counting approaches for classifying stochastic time histories. Fryba /1/ proposed several counting techniques for classifying time varying history. However, in this research, the rainflow counting method (RFCM) is implemented for determining cycle range.

*Rainflow counting method*

The rainflow cycle method of counting is perhaps the most commonly used approach for characterizing the irreversible stress elements of the stress-strain diagram which are critical for structural fatigue. It also detects stress range cycles related to low frequency components, as well as the mean stress involved with every cycle. The underlying principle involving identification of any stress cycle is to treat the section of a stress time history  $\sigma_r(x,t)$  between any of the two successive localised peaks being a half-cycle. The basic aspect involving rainflow counting approach is that fatigue damage caused by tiny stress cycles can be coupled with the fatigue damage caused by the larger ones. According to Fig. 6, if somehow the cycle 1-4 is disrupted by a little cycle 2-3-2', the position of point 2' is extremely close to point 2, and the material behaves as if no disruption through an additional cycle occurred.

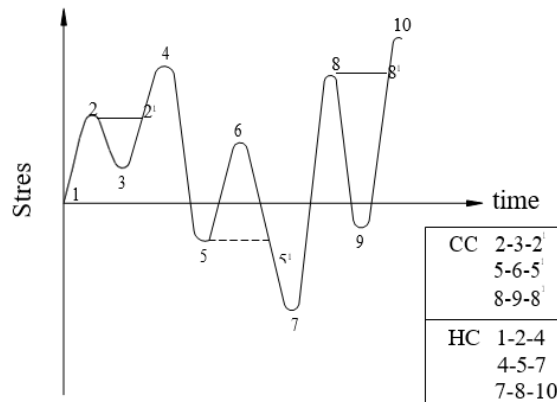


Figure 6. Stress-time history (CC-complete cycles, HC-half cycles).

*Stress counting principle*

The term 'rainflow' comes from an illustration of water that flows down a pagoda-shaped roof. The stress time history is flipped by 90 degrees to generate one such pagoda-shaped roof, as depicted in Fig. 7. The rules that have to be followed for stress counting are as follows.

- (1) As water goes from the starting stress towards the maximum, it counts one stress range, whereby it falls downhill across the next roof slope towards the next peak value.

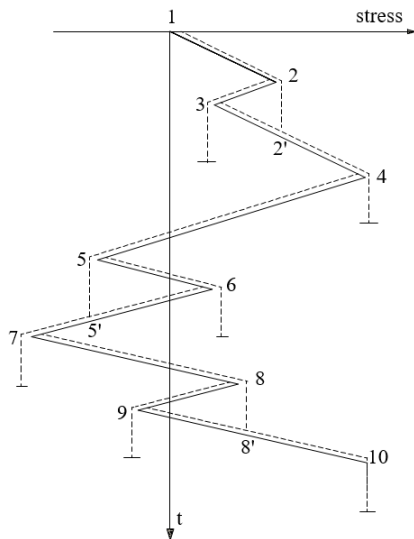


Figure 7. Stress time history (rotated).

The flow of the water is ceased if:

- (a) the lowest stress is less as compared to original stress;
  - (b) it comes into contact with some previous rain-flow;
  - (c) it approaches the strain record's ending.
- (2) The stress range is calculated as water moves downhill along the roof towards the next minimum, then subsequently down towards the next roof slope and towards the nearest minimum. It halts under following conditions:
- (a) the stress maxima exceed the original maximum;
  - (b) it makes contact with some previous rainflow;
  - (c) it has reached the conclusion of the record.
- (3) Roof portions that have not yet been counted by the rain-flow are measured as:
- (a) as explained in rule (2), the flow begins in the maximum and flows down over the succeeding minima, or
  - (b) as stated in rule (1), the flow begins in the minimum and flows down over the subsequent maximum. In either situation, the flow comes to a halt whenever
  - (c) it comes into contact with a previous stress that is more intense than the flow's starting point, or whenever
  - (d) it connects with a previous flow.

**Counting procedure**

The rainflow counting algorithm has been presented here using stress cycle diagram as shown in Figs. 8a and 8b.

- (1) The localised maxima  $A(0), A(1), \dots, A(k)$  are retrieved and processed from the stress time history.
- (2) The acquired collection of localised peaks is dissected into half- and full cycles.
- (3) The criteria involving cycle counting are given using the following:

$$A(i-1) \leq A(i+1) < A(i) \leq A(i+2), \tag{21}$$

$$A(i-1) \geq A(i+1) > A(i) \geq A(i+2). \tag{22}$$

- (4) The analysis progresses from  $i = 1$  till  $i = k - 2$ , i.e., from lowest to highest. If criteria Eq.(21) or Eq.(22) are met, one cycle equals two half-cycles having the following range of stress,

$$S_r = |A(i) - A(i+1)|. \tag{23}$$

- (5) Maxima  $A(i)$  and  $A(i+1)$  are removed from the extremes sequencing and the series is revised.

- (6) The technique described in (4) and (5) is continued till at least one cycle of the existing sequence exists.
- (7) When the cycle decomposition is finished, the stress ranges of the remainder series are referred to as half-cycles.
- (8) During the computations, the cycles and residual half-cycles of similar magnitude get merged. The final outcome is a list of stress range frequencies, which is commonly expressed as a frequency histogram and is referred to as a stress range spectrum.

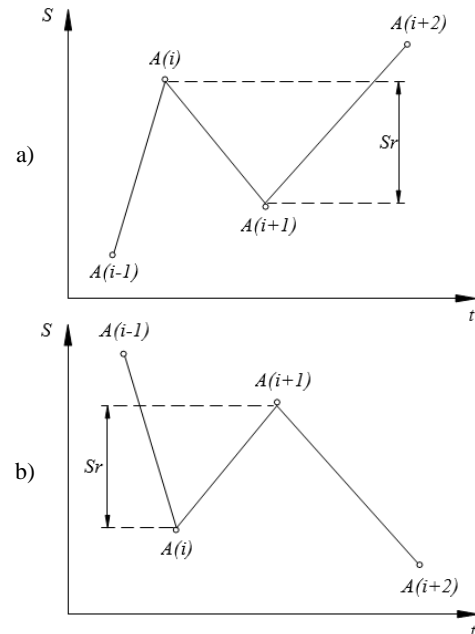


Figure 8. Two fundamental scenarios in full cycle counting of rainflow technique: a) ascending portion of time history; b) descending portion of time history.

**RESULTS AND DISCUSSION**

The numerical problem for fatigue analysis has been taken from Kermani and Waldron /14/, wherein the ends are simply supported. The steel bridge has a span length of 30 metres and radius of curvature 30.48 metres. Figure 9 depicts the cross-section of the bridge, whereas the sectional properties are listed in Table 2.

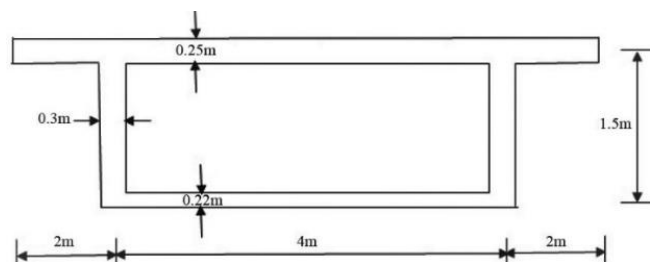


Figure 9. Cross-section of bridge.

Table 2. Sectional properties.

Sectional property	Value
$E$	$2.068 \times 10^{11} \text{ N/m}^2$
$\nu$	0.30
$G$	$7.997 \times 10^{10} \text{ N/m}^2$
$I_z$	$1.606 \text{ m}^4$
$J_T$	$3.259 \text{ m}^4$
$J_I$	$0.793 \text{ m}^6$

$J_{II}$	1.013 m <sup>6</sup>
$J_d$	0.005 m <sup>2</sup>
$\mu$	0.365
$A$	3.705 m <sup>2</sup>

*Stress-time history*

The fast moving train, as it passes over the bridge produces stresses like flexural stress, distortional warping stress, and torsional warping stress. The intensities for flexural stresses predominate all the other stresses in the current study for the bridge’s specified characteristics. As a result, only flexural stresses have been included for determining fatigue life of the bridge. Figures 10-12 show the variation of bending stresses for different span lengths, different vehicle velocities, and different rail surface irregularities, respectively. The highest stress values have been found for a span length of 15 m, velocity 450 km/h, and Class 6 rail surface irregularity.

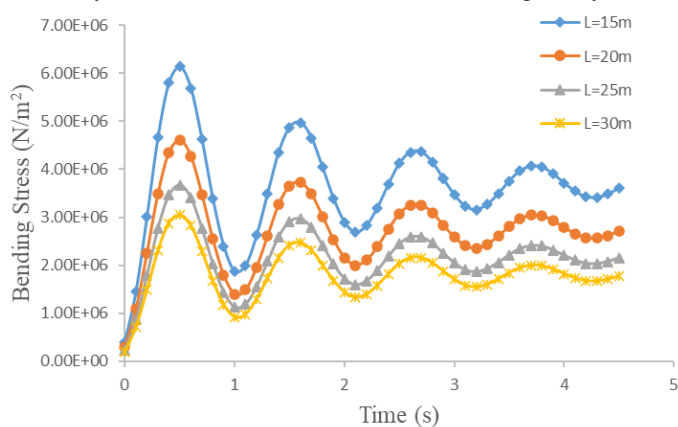


Figure 10. Stress-time for different span length.

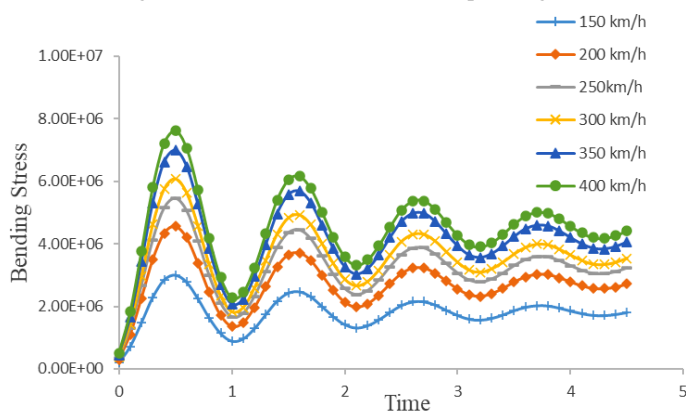


Figure 11. Stress-time for different velocity.

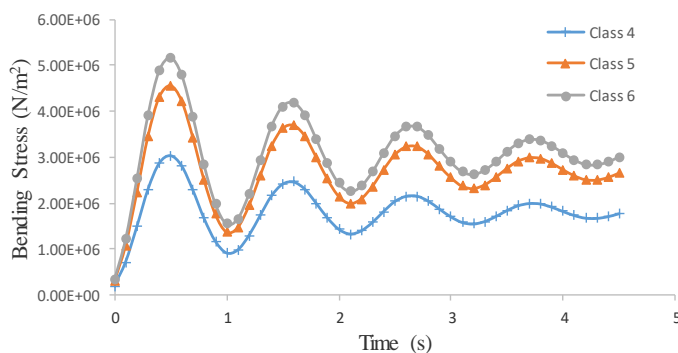


Figure 12. Stress-time for different rail surface irregularity.

PARAMETRIC STUDY

In this segment, the impact of critical parameters that govern the fatigue life of the box-girder bridge has been investigated. Following are some of the major factors that affect the fatigue life: span length; velocity; rail irregularity; fatigue constant.

*Effect of span length*

The variation in fatigue life as well as damage index is shown in Table 3, where span length is varied from 15 to 30 metres. It is clearly seen that as the span increases, the fatigue life of the bridge increases and the damage index decreases.

Table 3. Fatigue life variation with span length.

Span length (m)	Damage index	Fatigue life (years)
15	0.0079	126.26
20	0.0059	287.35
25	0.0041	320.51
30	0.0036	277.78

*Effect of velocity*

The variation of fatigue life and damage index with velocity varying from 150 to 400 km/h is shown in Table 4. An investigation into the Table goes to show that as velocity increases, the fatigue life of the bridge decreases and the damage index increases.

Table 4. Fatigue life variation with velocity.

Velocity (km/h)	Damage index	Fatigue life (years)
150	0.0025	396.82
200	0.0028	362.31
250	0.0031	320.51
300	0.0036	277.78
350	0.0042	238.09
400	0.0054	185.18

*Effect of rail irregularity*

Table 5 shows the effect of different classes of rail irregularity on the fatigue life and damage index of the bridge. Class 4, 5 and 6 indicate good, moderate, and poor condition of rail irregularity, respectively. It can be concluded that Class 4 rail irregularity has the maximum value of fatigue life, whereas the damage index is maximum for Class 6 rail irregularity.

Table 5. Fatigue life variation with rail irregularity.

Rail irregularity	Damage index	Fatigue life (years)
Class 4 (good)	0.0036	277.78
Class 5 (moderate)	0.0044	225.22
Class 6 (poor)	0.0054	185.18

*Effect of fatigue constant (K)*

The influence of different fatigue constant values on the fatigue life and damage index of the bridge is highlighted in Table 6. It is observed that as the fatigue constant values decrease, the fatigue life decreases and the damage index increases.

Table 6. Fatigue life variation with rail irregularity.

Detailed categ. AASHTO specs. 1998	Fatigue const. (K)	m (const.)	Damage index	Fatigue life (years)
A	250e+8	3	0.0036	277.78
B	120e+8	3	0.0075	133.33

B'	61e+8	3	0.0148	67.78
C	44e+8	3	0.0205	48.89
D	22e+8	3	0.0409	24.44
E	11e+8	3	0.0818	12.22

## CONCLUSION

The rainflow approach is widely considered as a technique that leads to superior fatigue life analysis because it can detect events in a complicated stress sequence that are consistent with steady-amplitude fatigue data. In this article, this technique is applied for predicting the fatigue life of a box girder bridge while taking into account its complex dynamic interactions with a fast moving train. The time history of bending stress with varying span length, velocity and rail surface irregularity has also been conducted. Furthermore, a parametric study has been done depicting the influence of different parameters on fatigue life and damage index of the box-girder bridge. Following points highlight the key aspects of the work.

The maximum values of bending stress are obtained for a span length of 15 m, a velocity of 400 km/h, and Class 6 rail surface irregularity.

The fatigue life of the bridge increases as the span increases, whereas the damage index decreases.

According to the findings, as the velocity increases, the fatigue life of the bridge drops and the damage index rises.

It is established that Class 4 rail irregularity has the highest fatigue life, while Class 6 rail irregularity has the highest damage index.

It has been found that fatigue life falls, and the damage index rises with the decreasing fatigue constant values.

## REFERENCES

- Fryba, L., Dynamics of Railway Bridges, 2<sup>nd</sup> Ed., Academia Praha, Thomas Telford, 1996.
- Li, Z.X., Chan, T.H.T., Ko, J.M. (2001), *Fatigue damage model for bridge under traffic loading: application made to Tsing Ma Bridge*, Theor. Appl. Fract. Mech. 35(1): 81-91. doi: 10.1016/S0167-8442(00)00051-3
- Repetto, M.P. (2005), *Cycle counting methods for bi-modal stationary Gaussian processes*, Probab. Eng. Mech. 20(3): 229-238. doi: 10.1016/j.probenmech.2005.05.004
- Mohammadi, J., Guralnik, S.A., Polepeddi, R. (1998), *Bridge fatigue life estimation from field data*, Pract. Period. Struct. Des. Constr. 3(3): 128-133. doi: 10.1061/(ASCE)1084-0680(1998)3:3(128)
- Leander, J., Karoumi, R. (2013), *Dynamics of thick bridge beams and its influence on fatigue life predictions*, J Constr. Steel Res. 89: 262-271. doi: 10.1016/j.jcsr.2013.07.012
- Lee, Y.J., Cho, S. (2016), *SHM-based probabilistic fatigue life prediction for bridges based on FE model updating*, Sensors, 16(3): 317. doi: 10.3390/s16030317
- Leitner, B., Figuli, L. (2018), *Fatigue life prediction of mechanical structures under stochastic loading*, In: MATEC Web Conf. 157: 02024. doi: 10.1051/mateconf/201815702024
- Macho, M., Ryjáček, P., Matos, J. (2019), *Fatigue life analysis of steel riveted rail bridges affected by corrosion*, Struct. Eng. Int. 29(4): 551-562. doi: 10.1080/10168664.2019.1612315
- Kourehli, S.S., Ghadimi, S., Ghadimi, R. (2020), *Application of dynamic kinetic energy and artificial neural network to crack identification in beams under moving mass*, Sharif J Civ. Eng. 35.2(4.2): 97-106. doi: 10.24200/j30.2018.50261.2293
- Bedi, R., Singh, S.P. (2020), *Flexural fatigue analysis of fibre reinforced polymer concrete composites under non-reversed loading*, Int. J Mater. Struct. Integr. 14(1): 1-21. doi: 10.1504/IJMSI.2020.107296
- Bertolesi, E., Buitrago, M., Adam, J.M., Calderón, P.A. (2021), *Fatigue assessment of steel riveted railway bridges: Full-scale tests and analytical approach*, J Constr. Steel Res. 182: 106664. doi: 10.1016/j.jcsr.2021.106664
- Kuncham, E., Sen, S., Kumar, P., Pathak, H. (2022), *An online model-based fatigue life prediction approach using extended Kalman filter*, Theor. Appl. Fract. Mech. 117: 103143. doi: 10.1016/j.tafmec.2021.103143
- Su, Y.H., Ye, X.W., Ding, Y. (2022), *ESS-based probabilistic fatigue life assessment of steel bridges: Methodology, numerical simulation and application*, Eng. Struct. 253: 113802. doi: 10.1016/j.engstruct.2021.113802
- Kermani, B., Waldron, P. (1993), *Analysis of continuous box girder bridges including the effects of distortion*, Comp. Struct. 47(3): 427-440. doi: 10.1016/0045-7949(93)90238-9

© 2023 The Author. Structural Integrity and Life, Published by DIVK (The Society for Structural Integrity and Life 'Prof. Dr Stojan Sedmak') (<http://divk.inovacionicentar.rs/ivk/home.html>). This is an open access article distributed under the terms and conditions of the [Creative Commons Attribution-NonCommercial-NoDerivatives 4.0 International License](#)